Elemental deportment and chemical structure evolution of iron ore during direct reduction in hydrogen atmosphere

*Tao Kan [a] *, Vladimir Strezov [a], Tim Evans [a], Frederick Theiss [b], Ray Frost [b]*

[a] Department of Environmental Sciences, Faculty of Science and Engineering, Macquarie University, Sydney NSW 2109, Australia

[b] School of Chemistry, Physics and Mechanical Engineering, Science and Engineering Faculty, Queensland University of Technology, GPO Box 2434, Brisbane, Queensland 4001, Australia

*Corresponding author. E-mails: tao.kan@mq.edu.au.

ABSTRACT

Direct reduced iron (DRI) technologies for iron production have been developed as an alternative route for direct iron ore reduction with a reductant gas, alleviating the need for separate cokemaking and sintering. This study aimed to provide an insight into the DRI production using H_2 in terms of elemental content change and chemical structure evolution for improved environmental control of the process. In this work, goethite sample was treated from room temperature to 1000 °C in 10 vol% H_2 in helium in a fixed-bed reactor. The investigated elements were divided into three groups: i) major elements (Fe and Al), ii) alkali and alkaline earth metal elements (mainly Na, K and Ca), iii) transition and post-transition metals (Ni, Cu, Zn, Pb, Cd, etc.) and iv) non-metal and metalloid elements (P, S, As, etc.) The elemental changes of iron ore with temperature were firstly determined by X-ray fluorescence (XRF) analysis and inductively coupled plasma–mass spectrometry (ICP-MS). X-ray diffraction (XRD), Fourier-transform infrared spectroscopy (FT-IR) and Raman spectrometry were employed to confirm the reactions and investigate the iron ore's chemical changes during the direct reduction. XRD analysis indicated the stepwise reduction of goethite → hematite → magnetite → wustite for the goethite sample. FT-IR and Raman spectrometry revealed the transformation of chemical groups with temperature. Results showed that no obvious changes could be noticed after heating the sample to 200°C in terms of the elemental contents and chemical structure. Further treatment of the sample to 500°C and subsequently 1000°C resulted in the content changes of some elements due to the weight loss of hydrated water by heating and reduction of the ore sample, respectively.

KEYWORDS: *Direct reduction of iron ore (DRI); Hydrogen; Temperature; Elemental contents; Chemical structure*

1. INTRODUCTION

It is predicted that the global steel production will double during 2012–2050 due to the higher demand primarily from developing countries (Pauliuk et al., 2013; Vogl et al., 2018). Around 60% of the global pig iron production is produced by the traditional iron processes involving iron oxide reduction in a blast furnace (BF). The BF process, where the required heat and reducing agents are supplied by the incomplete combustion of coke, is highly energy and emissions (e.g., SO_x, NO_x, particulate matters and VOCs) intensive with significant investments (Kan et al., 2016; Luo et al., 2011). Technical

transformation in non-blast furnace technologies, which are independent of metallurgical coke production, have been developed to fulfill the future market, such as direct reduction of iron ore (DRI) which has been increasingly attracting research and commercialisation efforts. A DRI process uses gas or solid reductant (e.g., coal, H_2 and/or CO) to directly reduce the iron ore to metallic iron under softening temperatures, featuring the advantages of improved energy saving and environmental performance mainly due to the elimination of coking and sintering (Man et al., 2014a; Man et al., 2014b). Although in the foreseeable future, the BF will continue to dominate the worldwide ironmaking market, the DRI production will be steadily increasing.

Many research efforts have been devoted to different aspects of the DRI process. Dilmac et al. (2015) investigated the direct reduction mechanism of Attepe iron ore with hydrogen in a fluidized bed, and found that the reduction process involved two stages consisting of low reduction controlled by nucleation of wustite and formation of metallic iron layers by gas/solid reaction at metallic iron/wustite interface. The operation stability for DRI is also significant. To avoid the defluidisation caused by sticking tendency of DRI particles in a fluidised bed, a two-step process coupling carbon precipitation reaction with reduction reaction of fine iron ore in a H_2-CO atmosphere was developed to modify the ore surface and thus cohesive force among DRI particles (Zhang et al., 2014). Studies have also been performed to investigate the effects of the reducing agent types and composition on the DRI process performance. Reduced Iron ore concentrate was reduced under H_2 and CO atmospheres and observed that the mass loss was not significantly affected by atmosphere below 800°C and H_2 enabled higher reduction rate than CO above 900 °C. The promotion of reduction by H_2 was attributed to the formation of porous and fibrous iron (Man & Feng, 2016) .

More research is still required on the change of iron ore properties under H_2 atmosphere. The behavior of elements (especially those of environmental concerns) in iron ore during reduction is of great interest and needs exploration. Previously, we investigated the trace element deportment and particle formation behaviour during DRI process in a circulating fluidised bed (CFB) reactor under H_2 atmosphere with emphasis on the risk assessment (Kan et al., 2015). This work aimed to evaluate the evolution of elements especially the heavy metals and chemical structure during reduction under H_2 with temperature. The raw goethite iron ore and the residual solids at 200, 500 and 1000 °C were characterised by various methods, including X-ray fluorescence (XRF), inductively coupled plasma–mass spectrometry (ICP-MS), X-ray diffraction (XRD), Fourier-transform infrared spectroscopy (FT-IR), and Raman spectrometry. This research will provide an insight into the environmental and process performance of an industrial DRI process, benefiting its further commercialisation.

2. EXPERIMENTAL

2.1. Iron ore sample and reduction process

The goethite iron ore sample with the chemical formula of FeO·(OH) used in this study was from Western Australia. The iron ore was crushed into powder (< 0.074 mm) and then subjected to programmed heating from room temperature to designated temperatures (200, 500, and 1000 °C) at 5 °C/min in a reductive atmosphere of 10 vol.% H_2 in He.

2.2 Elemental analysis

The elemental contents of the raw goethite and the reduction products at different temperatures were tested by two different methods. The concentrations of Na, Mg, Al, Si, P, S, Ca, Mn and Fe (in order of atomic weight) were analysed through Borate Flux bead sample preparation followed by Wavelength Dispersive X-ray fluorescence (XRF) spectrometry. Li, K, Sc, Cr, Co, Ni, Cu, Zn, Ga, Ge, As, Sr, Mo, Cd, Sn, Sb, Ba, La, Ce and Pb were tested through four acid digestion followed by inductively coupled plasma mass spectrometry (ICP-MS).

2.3 X-ray diffraction (XRD)

XRD was performed using a diffractometer (model: Malvern Panalytical Aeris) combining the 300 W high voltage generator operated at 40 kV/7.5 mA, the Empyrean X-ray tube Cu LFF and PIXcel1D line detector. The scans were carried out in the 2□ range of 10–70° at a step size of 0.04.

2.4 Fourier-transform infrared spectroscopy (FT-IR) and Raman spectrometry

2.4.1 FT-IR

A Nicolet iS50 FTIR spectrometer with Continuum IR microscope and in-built diamond ATR was employed to investigate the chemical functional groups of the samples. The FT-IR spectra were obtained over the 4000–400 cm^{-1} range with a resolution of 4 cm^{-1} and a data spacing of 0.482 cm^{-1}.

2.4.2 Raman spectroscopy

Raman spectra were collected using a Renishaw 1000 Raman microscope system equipped with a monochromator, filter system and a Charge Coupled Device (CCD) detector. Each sample was loaded on the stage of an Olympus BHSM microscope and focused before the microscope was switched to Raman mode. A HeNe laser (633 nm) at a nominal resolution of 2 cm^{-1} was employed to excite the Raman spectra with a range of 100–4000 cm^{-1}. GRAMS (Galactic Industries Corporation, NH, USA) software package was used to perform the baseline correction/adjustment and smoothing of FT-IR and Raman spectra.

3. RESULTS AND DISCUSSION

3.1 Behavior of elements during reduction

3.1.1 Mass remaining ratio (%)

Elemental analysis of the goethite and the processed samples at different temperatures (200, 500 and 1000°C) were performed to study the deportment of elements during direct reduction of the goethite. The results are presented in Table 1 in which the studied elements are divided into 6 major groups based on the periodic table: metalloid, other non-metals, alkali and alkaline earth metals, transition metals, post-transition metals, and lanthanoids. In each group, the elements are listed in order of atomic weight.

Table 1. Elemental contents of raw and reduced iron ore samples.

Groups of elements	Elements	Contents (mg/kg)			
		GL-raw	GL-200	GL-500	GL-1000
Metalloids	Si	10000	10300	11100	11500
	Ge	4.2	4.4	4.6	5
	As	nd	5	nd	nd
	Sb	1	0.9	1.1	0.6
Other non-metals	P	970	950	1100	1200
	S	70	70	40	10
Alkali and alkaline earth metals	Li	0.7	0.7	0.8	0.7
	Na	nd	200	nd	100
	Mg	800	800	1000	1000
	K	24	24	32	39
	Ca	200	200	300	200
	Sr	1.7	1.6	2.1	2.3
	Ba	3.8	4.4	4.4	4.6
Transition metals	Sc	0.8	0.9	0.9	0.9

	Cr	5	5	9	12
	Mn	900	870	970	1000
	Fe	601000	596000	655000	703000
	Co	nd	2	2	2
	Ni	7	7	6	9
	Cu	5	5	5	5
	Zn	15	26	20	56
	Mo	1.1	1.3	1.8	1.4
	Cd	nd	nd	nd	nd
	Al	5900	6300	6800	6900
	Ga	0.8	0.8	0.8	1
	Sn	1	3	1	1
Post-transition metals	Pb	0.9	1.1	1.3	nd
	La	2.7	2.8	3	3.4
Lanthanoids	Ce	8.5	8.6	9.1	10.3

Note: nd means 'not detected'.

As observed from Table 1, for the raw goethite sample (the 3rd column), Fe (in group of transition metals) was the most abundant element with a concentration of 601000 mg/kg (i.e., 60.1 wt%) followed by Si (10000 mg/kg, metalloid), Al (5900 mg/kg, post-transition metals), Mg (800 mg/kg, alkali and alkaline earth metal), P (970 mg/kg, other non-metal), Mn (900 mg/kg, transition metals) and Ca (200 mg/kg, alkali and alkaline earth metal). Some impurity elements especially the heavy metals with environmental pollution concerns, such as As, S, Cr, Cd and Pb were also tested. As and Pb in the raw sample were not detected due to their extreme trace amounts below the equipment detection limit or possible non-existence. Generally, there were no obvious changes in the contcentrations of most elements at reduction T = 200 °C, compared to the raw goethite.

When the temperature was further increased to 500°C and further to 1000 °C, there was an increase in the concentration for most elements, which should be mainly caused by the loss of sample mass due to the removal of moisture and oxygen element. For example, the Fe content was 60.1%, 59.6%, 65.5% and 70.3% corresponding to the GL-raw, GL-200, GL-500 and GL-1000, respectively. The increase in temperature from 200 to 500 °C induced decrease in the S content from 70 to 40 mg/kg. Further increase of temperature to 1000 °C resulted in a sharp drop to 10 mg/kg. This indicated that the evaporation of S took place between 200–500 °C and a higher temperature enhanced its evaporation from the solid matrix. A decrease in the Sb content from 1.1 to 0.6 mg/kg was also noticed when increasing the temperature from 500 to 1000 °C. Noticeably, the evolution of Pb was not obvious at 500 °C, however, Pb was almost removed when heating the goethite to 1000 °C.

To present the changing trends of elements with reduction temperature, the remaining mass ratio of each element (%, relative to the GL-raw) was presented in Table 2 by taking into account both of the elemental contents (Table 1) and the recorded remaining mass of the samples at different temperatures. The data in Table 2 represents the absolute mass of each element for a certain amount (i.e., 100) of the raw sample. Generally, the values for most elements are around 100% with acceptable errors, which indicate that these non-volatile elements remained in the solid sample. Results showed that 50% of Sb remained in the solid at T = 1000 °C, while with respect to S, about 50% retained in the solid at 500 °C with only 12% at 1000 °C.

Table 2. Remaining mass ratio (%) of elements in reduced samples.

Groups of elements	Elements	Remaining mass ratio of elements (%, relative to raw sample)			
		GL-RAW	GL-200	GL-500	GL-1000
Metalloid	Si	100	100.8	97.9	96.1
	Ge	100	102.6	96.6	99.5
	As	100	NA	NA	NA
	Sb	100	88.1	97.0	50.1
Other non-metal	P	100	95.9	100.0	103.4
	S	100	97.9	50.4	11.9
Alkali and alkaline earth metal	Li	100	97.9	100.8	83.6
	Na	100	NA	NA	NA
	Mg	100	97.9	110.3	104.5
	K	100	97.9	117.6	135.8
	Ca	100	97.9	132.3	83.6
	Sr	100	92.1	109.0	113.1
	Ba	100	113.4	102.1	101.2
Ttransition metals	Sc	100	110.1	99.2	94.0
	Cr	100	97.9	158.8	200.6
	Mn	100	94.6	95.1	92.8
	Fe	100	97.1	96.1	97.7
	Co	100	NA	NA	NA
	Ni	100	97.9	75.6	107.4
	Cu	100	97.9	88.2	83.6
	Zn	100	169.7	117.6	312.0
	Mo	100	115.7	144.3	106.4
	Cd	100	NA	NA	NA
Post-transition metals	Al	100	104.5	101.7	97.7
	Ga	100	97.9	88.2	104.5
	Sn	100	293.7	88.2	83.6
	Pb	100	119.6	127.4	NA
Lanthanoids	La	100	101.5	98.0	105.2
	Ce	100	99.0	94.4	101.3

Note: NA means ‘not applicable’.

3.1.2 Reduction degree of iron ore

The reduction degree (RD, %) of iron ore can be calculated as the mass of oxygen element removed during reduction divided by the total mass of oxygen in iron oxides in the raw ore (Dilmac et al., 2015;

Yi et al., 2013). The reducible oxygen content of the gangue materials by H_2 can be neglected due to their small amounts relative to the much larger amount of iron element (Chen et al., 2015; Yi et al., 2013; Yi et al., 2015). As shown in Table 1, the elements of major amounts on dry basis, including Fe, Si, Al, Mg, P, Mn and Ca, have been listed. Thus, the oxygen content of each sample can be calculated by difference, and RD is subsequently determined by the following equation:

$$RD\ (\%) = (M_0 - M_T)/M_0*100 = (C_0 - C_T*_T)/C_0*100$$

Where M_0 is the oxygen mass in the original iron ore, M_T is the oxygen mass in the ore processed at temperature T (T = 200, 500 and 1000 °C), C_0 is the oxygen content of the original iron ore, C_T is the oxygen content of the ore processed at temperature T, R_T is the mass ratio of the ore processed at temperature T to the original iron ore.

At T = 200 °C, the processed goethite did not show any obvious oxygen removal and the reduction degree is zero. The calculation results indicated the RD of 24.9% and 39.6%, respectively, for the goethite processed at T = 500 and 1000 °C. Obviously, the increase in the reduction temperature led to a higher RD.

3.2 Crystalline phase by XRD

XRD allows the phase identification of iron ores at different reduction temperatures, as shown in Figure 1.

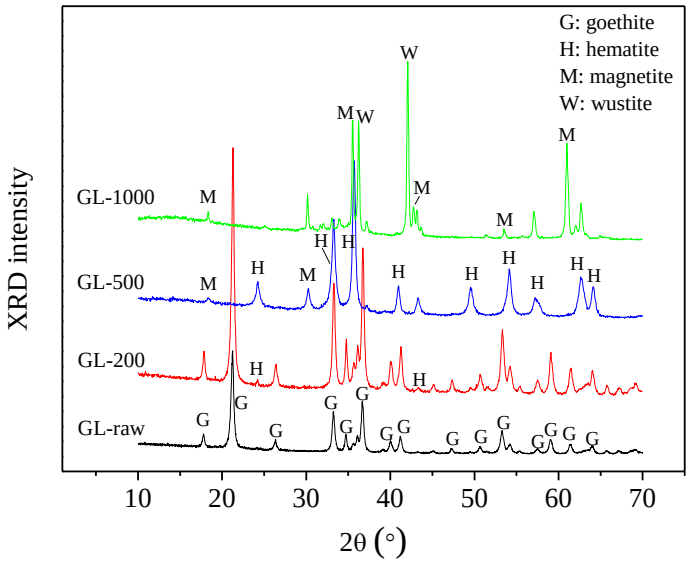

Figure 1. XRD patterns of iron ore reduced at different temperatures.

The XRD pattern of GL-raw sample consists of typical goethite peaks, which was well consistent with previous studies (Liu et al., 2013). Compared to GL-raw, GL-200 did not exhibit much difference in the peak positions except for the negligible peaks for the hematite. When increasing the temperature from 200 to 500°C, all the goethite peaks disappeared and they were replaced by hematite peaks due to the formation of hematite through dehydroxylation Reaction 1 (Liu et al., 2004). The characteristic peaks of magnetite could also be observed as a result of the partial reduction of hematite (Reaction 2) (Oh & Noh, 2017).

$FeO(OH)\ (goethite) \rightarrow \alpha\text{-}Fe_2O_3\ (hematite)$ Reaction 1

$\alpha\text{-}Fe_2O_3\ (hematite) + H_2 \rightarrow Fe_3O_4\ (magnetite) + H_2O$ Reaction 2

$Fe_3O_4\ (magnetite) + H_2 \rightarrow FeO\ (wustite) + H_2O$ Reaction 3

Generally, the reduction of hematite to magnetite could start below 530 °C and completed at around 620–670 °C (Liu et al., 2004). As shown in the XRD pattern of GL-1000, the phases were a mixture of magnetite and wustite with some amount of remaining hematite when raising the reduction temperature to 1000 °C. The identification of magnetite and wustite peaks was in accordance to other published works (Yi et al., 2015). The formation of wustite was expressed as Reaction 3, which takes place at a temperatures above 570 °C (Schenk, 2011).

3.3 Chemical structure by FT-IR and Raman spectrometry

3.3.1 FT-IR results

The functional groups of the raw and reduced ore at different temperatures were determined by the FT-IR spectra, as shown in Figure 2.

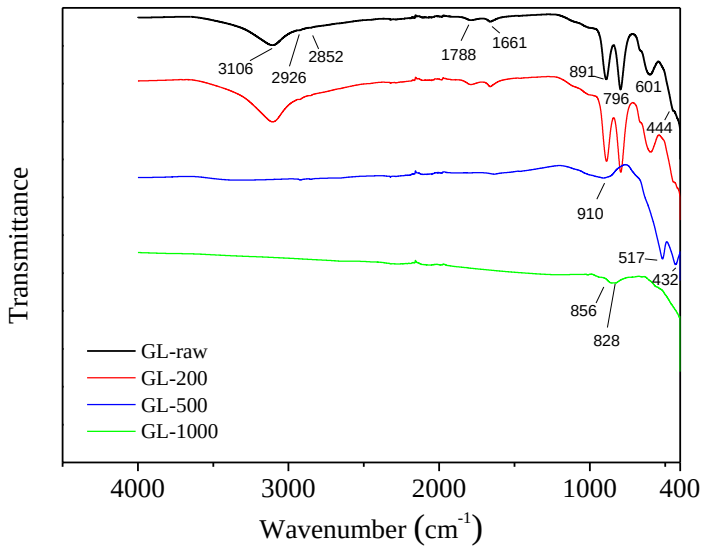

Figure 2. FT-IR spectra of iron ores reduced at different temperatures.

For the GL-raw sample, the peaks at 444 cm^{-1} indicated the presence of kaolinite and/or hematite (Schiavon, 2007; Strezov et al., 2010) and 601 cm^{-1} was possibly due to sulphate (Salama et al., 2015). The goethite structure was confirmed by the strong peaks at 796 and 891 cm^{-1} corresponding to O=Fe–O–H vibrations (Strezov et al., 2010). The existence of organic structures was also identified. The band at 1788 cm^{-1} was possibly caused by the presence of nitrate (Salama et al., 2015). The broad absorption band centring at around 3106 cm^{-1} corresponded to the stretching of the OH group and bonded water (Strezov et al., 2010).

When processing the GL at 200 °C (GL-200), all the IR peaks remained unchanged. With further increase of the temperature to 500 °C almost all bands disappeared as a result of transformation of goethite to hematite. The emerging peaks at 432 and 517 cm^{-1} were a result of the formation of hematite (Fe_2O_3) after heating (Strezov et al., 2010). The new band at 910 cm^{-1} was assigned to the hydroxyl deformation (Ruan et al., 2001), which was removed after heating the sample to 1000 °C. For the GL-1000, only a band at 828 cm^{-1} and a small side peak at 856 cm^{-1} was identified, which was ascribed to the quartz after the removal of other previous overlapping bands (Omran et al., 2015).

3.3.2 Raman spectroscopy results

Raman spectroscopy can provide complementary mineralogical characterisation to infrared spectroscopy. Figure 3 presents the Raman spectra of the iron ore processed at different final temperatures under reducing condition.

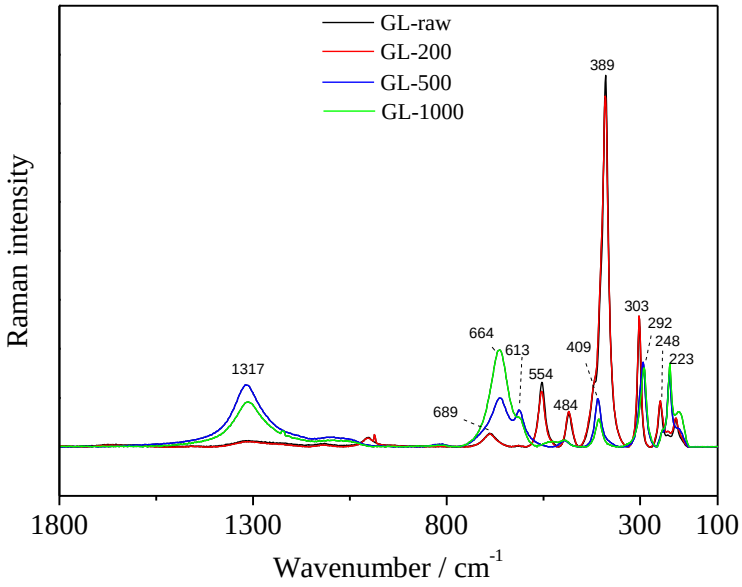

Figure 3. Raman spectra of iron ores processed at different final temperatures.

The Raman spectrum of the GL-raw featured a wide and weak band at around 1317 cm^{-1}, small peaks at 689, 554, 484 and 248 cm^{-1}, and strong peak at 389 cm^{-1} followed by medium peak at 303 cm^{-1}. All the identified peaks arose from the goethite with the most outstanding peak at 389 cm^{-1} corresponding to Fe-O-Fe/-OH symmetric stretching, which aligned well with the Raman profile of the goethite in previous studies (de Faria & Lopes, 2007; Liu et al., 2013). GL-200 had a similar Raman profile as the GL-raw. After reducing the GL at 500°C, the sample exhibited different Raman profile with observed peaks at 1317, 613, 409, 292 and 223 cm^{-1} arising from hematite (Chamritski & Burns, 2005; Kremer et al., 2012; Smith et al., 2017), which is in accordance with the FTIR results of GL-500. The peak at 664 cm^{-1} was assigned to Fe-O symmetric stretching in magnetite (de Faria & Lopes, 2007; deFaria et al., 1997). The increase in temperature from 500 to 1000 °C resulted in the decline in the intensities of hematite peaks while the enhancement of the magnetite peak at 664 cm^{-1}, due to reduction of the iron ore at higher temperature.

4. CONCLUSION

In this study, one goethite iron ore (GL) was investigated during its reduction under 10% H_2 in He at different final temperatures of 200, 500 and 1000 °C. Elements' behavior, crystalline phases, chemical functional groups, surface morphology with reduction temperature were examined. Results showed that the reduction temperature of 200 °C did not have obvious effects on the iron ore properties while increasing the temperature to 500 °C and 1000 °C generated obvious changes. Most elements experienced increase in concentration when the temperature was increased from 200 to 500 °C and 1000 °C mainly as a result of enrichment in the solid structure while the hydroxyl and oxygen were lost during heating and reduction. The mass remaining ratios of the elements within the investigated temperature range generally kept constant at around 100%, with exception to some elements which were lost during heating and reduction due to their volatility. Compared to the raw iron ore, the contained Sb in the solid was greatly reduced by 50% while Pb was almost removed at 1000 °C. The S element was evaporated between 200-500 °C, remaining 50.4% and 11.9% at 500 and 1000 °C, respectively. XRD patterns

showed the stepwise reduction from goethite to wustite. The evolution of chemical groups with temperature was consistent with the XRD results.

ACKNOWLEDGEMENTS

The authors acknowledge the financial support of the Australian Research Council through the Linkage funding scheme. The paper was initially published in the Chemeca 2019 proceedings and copyrighted to Engineers Australia. We acknowledge Engineers Australia for granting permission to deposit our paper to Macquarie University open repository.

REFERENCES

Chamritski, I., Burns, G. 2005. "Infrared- and Raman-active phonons of magnetite, maghemite, and hematite: A computer simulation and spectroscopic study". *Journal of Physical Chemistry B*, **109**(11), pp 4965-4968.

Chen, F., Mohassab, Y., Jiang, T., Sohn, H.Y. 2015. "Hydrogen Reduction Kinetics of Hematite Concentrate Particles Relevant to a Novel Flash Ironmaking Process". *Metallurgical and Materials Transactions B-Process Metallurgy and Materials Processing Science*, **46**(3), pp 1133-1145.

de Faria, D.L.A., Lopes, F.N. 2007. "Heated goethite and natural hematite: Can Raman spectroscopy be used to differentiate them?". *Vibrational Spectroscopy*, **45**(2), pp 117-121.

deFaria, D.L.A., Silva, S.V., deOliveira, M.T. 1997. "Raman microspectroscopy of some iron oxides and oxyhydroxides". *Journal of Raman Spectroscopy*, **28**(11), pp 873-878.

Dilmac, N., Yoruk, S., Gulaboglu, S.M. 2015. "Investigation of Direct Reduction Mechanism of Attepe Iron Ore by Hydrogen in a Fluidized Bed". *Metallurgical and Materials Transactions B-Process Metallurgy and Materials Processing Science*, **46**(5), pp 2278-2287.

Kan, T., Evans, T., Strezov, V., Nelson, P.F. 2016. Risk Assessment and Control of Emissions from Ironmaking. in: *Ironmaking and Steelmaking Processes: Greenhouse Emissions, Control, and Reduction*, (Ed.) P. Cavaliere, Springer International Publishing. Cham, pp. 321-339.

Kan, T., Strezov, V., Evans, T.J., Nelson, P.F. 2015. "Trace element deportment and particle formation behaviour during thermal processing of iron ore: technical reference for risk assessment of iron ore processing". *Journal of Cleaner Production*, **102**, pp 384-393.

Kremer, B., Owocki, K., Krolikowska, A., Wrzosek, B., Kazmierczak, J. 2012. "Mineral microbial structures in a bone of the Late Cretaceous dinosaur Saurolophus angustirostris from the Gobi Desert, Mongolia - a Raman spectroscopy study". *Palaeogeography Palaeoclimatology Palaeoecology*, **358**, pp 51-61.

Liu, G.S., Strezov, V., Lucas, J.A., Wibberley, L.J. 2004. "Thermal investigations of direct iron ore reduction with coal". *Thermochimica Acta*, **410**(1-2), pp 133-140.

Liu, H.B., Chen, T.H., Zou, X.H., Qing, C.S., Frost, R.L. 2013. "Effect of Al content on the structure of Al-substituted goethite: a micro-Raman spectroscopic study". *Journal of Raman Spectroscopy*, **44**(11), pp 1609-1614.

Luo, S.Y., Yi, C.J., Zhou, Y.M. 2011. "Direct reduction of mixed biomass-Fe2O3 briquettes using biomass-generated syngas". *Renewable Energy*, **36**(12), pp 3332-3336.

Man, Y., Feng, J.X. 2016. "Effect of iron ore-coal pellets during reduction with hydrogen and carbon monoxide". *Powder Technology*, **301**, pp 1213-1217.

Man, Y., Feng, J.X., Chen, Y.M., Zhou, J.Z. 2014a. "Mass Loss and Direct Reduction Characteristics of Iron Ore-coal Composite Pellets". *Journal of Iron and Steel Research International*, **21**(12), pp 1090-1094.

Man, Y., Feng, J.X., Li, F.J., Ge, Q., Chen, Y.M., Zhou, J.Z. 2014b. "Influence of temperature and time on reduction behavior in iron ore-coal composite pellets". *Powder Technology*, **256**, pp 361-366.

Oh, J., Noh, D. 2017. "The reduction kinetics of hematite particles in H-2 and CO atmospheres". *Fuel*, **196**, pp 144-153.

Omran, M., Fabritius, T., Elmandy, A.M., Abdel-Khalek, N.A., El-Aref, M., Elmanawi, A. 2015. "XPS and FTIR spectroscopic study on microwave treated high phosphorus iron ore". *Applied Surface Science*, **345**, pp 127-140.

Pauliuk, S., Milford, R.L., Muller, D.B., Allwood, J.M. 2013. "The Steel Scrap Age". *Environmental Science & Technology*, **47**(7), pp 3448-3454.

Ruan, H.D., Frost, R.L., Kloprogge, J.T. 2001. "The behavior of hydroxyl units of synthetic goethite and its dehydroxylated product hematite". *Spectrochimica Acta Part a-Molecular and Biomolecular Spectroscopy*, **57**(13), pp 2575-2586.

Salama, W., El Aref, M., Gaupp, R. 2015. "Spectroscopic characterization of iron ores formed in different geological environments using FTIR, XPS, Mossbauer spectroscopy and thermoanalyses". *Spectrochimica Acta Part a-Molecular and Biomolecular Spectroscopy*, **136**, pp 1816-1826.

Schenk, J.L. 2011. "Recent status of fluidized bed technologies for producing iron input materials for steelmaking". *Particuology*, **9**(1), pp 14-23.

Schiavon, N. 2007. "Kaolinisation of granite in an urban environment". *Environmental Geology*, **52**(2), pp 333-341.

Smith, J.P., Smith, F.C., Booksh, K.S. 2017. "Spatial and spectral resolution of carbonaceous material from hematite (alpha-Fe2O3) using multi-variate curve resolution-alternating least squares (MCR-ALS) with Raman microspectroscopic mapping: implications for the search for life on Mars". *Analyst*, **142**(17), pp 3140-3156.

Strezov, V., Ziolkowski, A., Evans, T.J., Nelson, P.F. 2010. "Assessment of evolution of loss on ignition matter during heating of iron ores". *Journal of Thermal Analysis and Calorimetry*, **100**(3), pp 901-907.

Vogl, V., Ahman, M., Nilsson, L.J. 2018. "Assessment of hydrogen direct reduction for fossil-free steelmaking". *Journal of Cleaner Production*, **203**, pp 736-745.

Yi, L.Y., Huang, Z.C., Jiang, T. 2013. "Sticking of iron ore pellets during reduction with hydrogen and carbon monoxide mixtures: Behavior and mechanism". *Powder Technology*, **235**, pp 1001-1007.

Yi, L.Y., Huang, Z.C., Jiang, T., Wang, L.N., Qi, T. 2015. "Swelling behavior of iron ore pellet reduced by H-2-CO mixtures". *Powder Technology*, **269**, pp 290-295.

Zhang, T., Lei, C., Zhu, Q.S. 2014. "Reduction of fine iron ore via a two-step fluidized bed direct reduction process". *Powder Technology*, **254**, pp 1-11.

BIOGRAPHY

Dr Tao Kan was awarded the Ph.D degree in Chemistry from the University of Science and Technology of China. He worked as a Postdoctoral Fellow in the Chinese Academy of Sciences during 2010–2012 in the field of catalytic hydroprocessing of coal tar to generate clean gasoline and diesel. Afterwards, he joined Macquarie University, Australia, as a Research Fellow. His research interests are currently biomass pyrolysis and catalysis for energy generation as well as thermal processing of iron ore with emphasis on environmental pollution. Dr Kan's research has produced more than 50 publications, attracting more than 1000 citations.

Prof. Vladimir Strezov completed his PhD in Chemical Engineering at the University of Newcastle, Australia. Before joining Macquarie University in 2003 he was a research associate and laboratory manager at the University of Newcastle. He is currently Professor at the Department of Environmental Sciences at Macquarie University, Australia. Prof Strezov's current research projects are concerned with improvement of energy efficiency and reduction of emissions in minerals processing, electricity generation and production of biofuels. He has established close links with several primary industries leading to successful joint projects in the field of energy and sustainability.

Dr Tim Evans is Adjunct Professor at the Faculty of Science and Engineering, Macquarie University (Australia) and Principal Engineer at Rio Tinto. He has a long association with Australian primary industries, such as BHP Billiton, HIsmelt and Rio Tinto. He holds PhD in Chemical Engineering from the University of Newcastle. Dr Evans' expertise is in energy transformation and mineral processing, specifically high temperature industrial processing.

Dr. Frederick Theiss obtained his PhD at Queensland University of Technology in 2016 under the supervision of Emeritus Prof. Ray Frost and Prof. Godwin Ayoko. He is now working as a Research Assistant in the School of Chemistry, Physics and Mechanical Engineering (CPME) & School of Civil Engineering and Built Environment

(CEBE), Science and Engineering Faculty, Queensland University of Technology, Australia. His research interests mainly focus on the mineral synthesis and processing, layered double hydroxides, etc.

Emeritus Prof. Ray Frost completed his PhD at University of Queensland, Australia. He works in the disciplines of Physical Chemistry (incl. Structural) and Analytical Chemistry. He became a professor in 2005, and in now working in the School of Chemistry, Physics and Mechanical Engineering, Science and Engineering Faculty, Queensland University of Technology. Prof. Frost research interests include molecular assembly of hydrotalcites, nanochemistry of titania/zirconia/alumina phases, mineral zoning, molecular assembly in secondary minerals, intercalation of kaolinite, pillaring of montmorillonites, and molecular structure of minerals with more than 1200 research items.